AN ANALYSIS OF THE ELECTRON SPIN RESONANCE OF LOW SPIN FERRIC HEME COMPOUNDS

GILDA M. HARRIS LOEW

From the Department of Physics, Pomona College, Claremont, California 91711. Dr. Loew's present address is the Department of Genetics, Stanford University School of Medicine, Stanford, California 94305.

ABSTRACT The electron spin resonance spectra of low spin ferric heme proteins are calculated and compared with experimental spectra recently obtained for a large number of heme proteins. On the basis of observed g values, these heme proteins have been categorized into five prototypes. Since electron spin resonance spectra are quite sensitive to small changes in the local environment about the paramagnetic ion, we have explored in some detail, the possibility that the g value variation in these different types of proteins is due to systematic environmental changes. To this end, we have calculated the g values as a function of tetragonal and rhombic distortions and compared our results with observed behavior. In addition we have also calculated the energy intervals between the low spin states in zero magnetic field and the temperature dependent magnetic moments and studied the effect on these properties also of small symmetry changes.

INTRODUCTION

Recently, the low temperature electron spin resonance (esr) spectra of a very large number of ferric heme proteins has been investigated for which a signal typical of that from a doublet ground state of the ferric ion has been observed.[1] Literally hundreds of heme proteins and their derivatives have been observed including such proteins as hemoglobin A and M, separated chains of hemoglobin, cytochromes, peroxidases, catalases, and RHP and P450 bacterial heme proteins. Most of these heme proteins form a series of derivatives by replacement of the sixth ligand of the Fe and many of these have also been investigated. Of the hundreds of compounds studied, all have three distinct g values, indicative of some rhombic distortion in the local environment about the ferric ion. No axial or isotropic g values have thus far been observed in ferric heme proteins. All of these compounds have been classified

[1] W. Blumberg and J. Peisach, private communication. The work was done at Bell Telephone Laboratories and used here with the kind permission of the investigators.

TABLE I

EXPERIMENTAL g VALUES* FOR FIVE UNIQUE TYPES OF HEME PROTEINS

Type	Example	Number of compounds	g_z	g_y	g_x
c-type	Cytochrome *c*	25	3.15	2.25	1.25
b-type	Cytochrome *b*; salycylate Hb	50	2.95	2.26	1.47
h-type	Histidine Hb	100	2.80	2.26	1.67
o-type	(OH) Hb, Mb	150	2.55	2.17	1.85
p-type	P450; pyridine Hb	∿100	2.41	2.26	1.93

* This work was done by W. Blumberg and J. Peisach, Bell Telephone Laboratories, and reproduced here with the kind permission of the authors.

into one of five types according to their g values since of all compounds studied, only five different sets of g values have thus far been observed.[1]

Table I gives the g values for the five types of heme proteins and the name of a prototype compound for which these values have been observed. Also listed in this table are the number of heme proteins observed of each type.

For another class of Fe proteins, the reduced form of plant type ferredoxins, the observed esr signal is also thought to be that of low spin ferric ion.[2] In these Fe-S compounds, both axial and rhombic g values have been observed. In each case two or three g values very close to 2 are observed. However, the nature and symmetry of the immediate environment about the Fe in these proteins and even the formal oxidation state of the Fe is not yet as well understood as for the heme proteins.

In the light of these recent experimental developments, we have made a general analysis of the g value variation to be expected for low spin ferric ion as a function of axial and rhombic distortion of a strong octahedral perturbation. In the work to be presented here, the model used and the results obtained are discussed and correlated with specific conformation and bonding changes possible in these compounds. With the same model, we are also able to account for the experimental esr data for the five types of low spin heme proteins given in Table I. Using the wave functions which characterize the g values, we have also calculated the energy separation between the low spin states in zero field, and the effective magnetic moments as a function of temperature to be expected from a thermal average of all the low spin states. These properties depend on the magnitude of the spin-orbit coupling as well as the extent of tetragonal and rhombic distortion.

GENERAL ANALYSIS

It has already been fairly well established that in a heme environment, ferric ion with a $3d^5$ free ion electron configuration can exist in a sextet or doublet ground state. A

[1] H. Beinert, University of Wisconsin, and I. Salmeen, University of Michigan. Private communication.

quartet state, while possibly fairly low-lying, does not appear to become the ground state in such compounds. It also seems fairly certain that the state which becomes the low spin ground state arises from a $^2T_2(t_2^5)$ strong cubic field manifold of states (1). We have in the past studied the conditions in crystal field parameter space under which sextet, quartet, and doublet states become the ground state (2). Also, since these states mix under spin-orbit coupling, there is a small symmetry-perturbation region where a substantially spin-mixed state can be the ground state. For the case of six equal ligands, i.e. octahedral symmetry, there is a certain minimum, rather substantial, overall perturbation necessary for a doublet ground state (2). If the axial ligands are weakened, thus causing an axial distortion of the environment, the over-all perturbation necessary for a doublet ground state increases (2). Conversely, if a system already exists in a doublet ground state, weakening the axial ligands can cause a change to a sextet ground state (2). For the compounds at hand the combination of average cubic perturbation and tetragonal distortion appears to be such that a doublet ground state is favored, since esr, typical of such a state, was observed at low temperatures.[1]

The doublet states can interact with excited sextet and quartet states. If such excited states were low-lying in these compounds, the ground state would in fact be a heavily spin-mixed state. We have in the past (3) calculated the g values to be expected in such a case and they do not correspond to the observed values. Therefore interactions with excited quartet and sextet states can be ignored in considering the behavior of the low-lying doublet states of $^2T_2$ in these compounds.

The six $^2T_2$ states to be considered here are given in Table II A, which labels the states by their symmetry and spin behavior in O_h, D_4, and D_4^* symmetry. These states are all degenerate in octahedral symmetry and hence the value of the cubic field strength need not be considered except to note that it must be greater than the minimum required for a low spin ground state. These six degenerate states interact among themselves under the influence of spin-orbit coupling, and a tetragonal and rhombic distortion of the local perturbing environment. They factor into two sets of three interacting states, three Kramer's doublets. The interaction matrix for the imaginary basis set of states given in Table II A is shown in Table II B. Diagonal and off-diagonal matrix elements are given in terms of two crystal field parameters, μ and

TABLE IIA

BASIS SET OF LOW SPIN STATES

ϕ_i	$\lvert Sh(O_h)m_s\theta\rangle$	$Sh(D_4)t\tau(D_4^*)$
1	$^2T_2$ (1, $-\frac{1}{2}$)	$^2EE''\alpha$
1′	$^2T_2$ (-1, $\frac{1}{2}$)	$^2EE''\beta$
2	$^2T_2$ (-1, $-\frac{1}{2}$)	$^2EE'\alpha$
2′	$^2T_2$ (1, $\frac{1}{2}$)	$^2EE'\beta$
3	$^2T_2$ (0, $\frac{1}{2}$)	$^2B_2$ $E''\alpha$
3′	$^2T_2$ (0, $-\frac{1}{2}$)	$^2B_2$ $E''\beta$

TABLE IIB

INTERACTION MATRIX OF BASIS SET OF STATES

	ϕ_1	ϕ_2	ϕ_3
ϕ_1	$-\delta/2 - E$	$\delta/\sqrt{2}$	$R/2$
ϕ_2	$\delta/\sqrt{2}$	$\mu - E$	0
ϕ_3	$R/2$	0	$+\delta/2 - E$

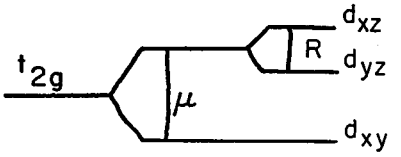

FIGURE 1 Crystal field parameters in terms of single orbital energy intervals.

R, and the spin-orbit coupling parameter δ. The parameter μ is a measure of the difference in bonding perturbation of the four in-plane porphyrin nitrogens and the two axial ligands lying along the z axis, while R is a measure of a rhombic distortion which distinguishes the x and y axes. We have defined these parameters in terms of the energy intervals between the one electron orbitals, d_{xy}, d_{xz}, and d_{yz}, a real basis set of t_{2g} orbitals, which are linear combinations of those in Table II A. This definition of μ and R is shown schematically in Fig. 1. All of our ensuing discussion shall be with positive values of μ and R. A positive value of μ implies axial ligands which are somewhat weaker than in-plane ligands and of the same sign. Positive and negative values of R simply interchange their role of the x and y axis and all results should be independent of the sign of R. The parameters μ and R can also be defined in terms of coefficients of certain terms in the crystal field potential of specific symmetries. In such a case both μ and R are found to be certain sums of quadratic and quartic coefficients. We have previously shown (4) how this is the case for D_4 symmetry and shall not pursue this analogy further here.

A solution of the interaction matrix given in Table II B for sets of values for the three parameters yields sets of three three-component doubly degenerate eigenfunctions of the form:

$$\psi_i = A_i \phi_1 + B_i \phi_2 + C_i \phi_3, \tag{1}$$

where ϕ_i are as labeled in Table II A, $i = 1$–3. A corresponding set of three energy eigenvalues is also obtained. It can be shown analytically that these three-component functions are uniquely determined by the ratio of any two of the parameters to a third and that the energy intervals are proportional to the third, e.g.:

$$\psi_i = \psi_i(\delta/\mu, \delta/R); \Delta E_{ik} = \delta \cdot \Delta E'_{ik}(\delta/\mu, \delta/R).$$

From the interaction matrix given in Table II B we see that states ϕ_1 and ϕ_2 mix

by spin-orbit coupling and are separated by the quantity $(\mu + \delta/2)$. Thus the mixing of state ϕ_2, i.e. the coefficient B, in the ground state decreases as the ratio δ/μ decreases. States ϕ_1 and ϕ_3 mix by a rhombic distortion and are separated by the value δ. Thus the mixing of state ϕ_3, i.e. the coefficient C, into the ground state increases as the quantity δ/R decreases.

In a magnetic field each of these three three-component doubly degenerate states is further split. However, only the ground state intra-doublet transition is seen in the electron spin resonance spectra. Using the magnetic field energy operators, $BH_j(L_j + 2S_j)$, $j = x$, y, and z with the states ψ_i, and defining the principal g values for any intradoublet transition as $g_j = \Delta E_j/BH_j$, these g values can be expressed in terms of the coefficients A, B, and C of the function ψ_i,

$$g_z = 2\,|2A^2 - B^2| \tag{2 a}$$

$$g_y = 2\,(-\sqrt{2}A + B)(\sqrt{2}C + B)\,| \tag{2 b}$$

$$g_x = 2\,(\sqrt{2}A - B)(\sqrt{2}C - B)\,|. \tag{2 c}$$

Using these expressions for the g values and the interaction matrix in Table II B, we have written a program for the IBM 360/2040 to calculate eigenfunctions, energy eigenvalues, and g values for specified sets of parameters. We have used this program to delineate g value and eigenfunction behavior for a wide range of axial and rhombic distortions. As we have mentioned, the ground and excited state wave functions and therefore the observed g values are uniquely determined by the ratio of any two of the parameters in the interaction matrix to the third. The two ratios chosen were δ/μ and R/μ and the range of values investigated for each were $\delta/\mu = 0.01 - 100$ and $R/\mu = 0 - 2$. This range is illustrated schematically in the diagram in Fig. 2 *a*. It is broad enough to include all the limiting symmetry and perturbation situations that

a

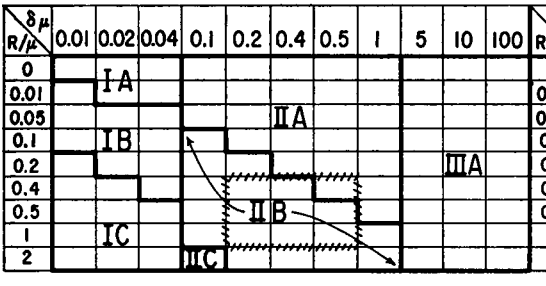

b

R/μ	10^2 400	10^2 200	10^2 100	10^1 400	10^1 200	10^1 100	800	400	80	40	4
0	0	0	0	0	0	0	0	0	0	0	0
0.01	400	200	100	40	20	10	8	4	0.8	0.4	0.04
0.05	200^1	100^1	500	200	100	50	40	20	4	2	0.2
0.1	400^1	200^1	100^1	400	200	100	80	40	8	4	0.4
0.2	800^1	400^1	200^1	800	400	200	160	80	16	8	0.8
0.4	100^2	800^1	400^1	100^1	800	400	320	160	32	16	1.6
0.5	200^2	100^2	500^1	200^1	100^1	500	400	200	40	20	2
1	400^2	200^2	100^2	400^1	200^1	100^1	800	400	80	40	4
2	800^2	400^2	200^2	800^1	400^1	200^1	100^1	800	160	80	8

FIGURE 2 Delineation of regions of axial and rhombic distortions in parameter space.
I. Strong tetragonal: A. weak rhombic; B. moderate rhombic; C. strong rhombic.
II. Moderate tetragonal: A. weak rhombic; B. moderate rhombic; C. strong rhombic.
IIIA. Weak tetragonal—weak rhombic (near-octahedral symmetry).
Definition: strong $> 10\delta$; $10\,\delta >$ intermediate $> \delta$; weak $< \delta$.
Superscript $n = \times 10^n$.

might reasonably occur in the ferric heme compounds. We have for the sake of discussion divided the parameter area considered into several subdivisions shown in Fig. 2 *a*. To do so, we define regions of strong, intermediate, and weak axial distortion, i.e., regions I, II, and III, in terms of the spin-orbit coupling parameter as follows: for strong axial perturbation $\mu > 10\delta$, for the intermediate case, $\delta \leq \mu \leq 10\delta$, and for the weak case, $\mu < \delta$. In addition we make the same sort of definition of strong, intermediate, and weak rhombic distortions: $R > 10\delta$, $\delta \leq R \leq 10\delta$, and $R < \delta$, thus delineating subregions A, B, and C in Fig. 2 *a*.

The question now arises as to what further information we can use to correlate the set of parameter ratios chosen with actual variations occurring in series of similar compounds. Of the three parameters used, the spin-orbit coupling, a property of the free ferric ion itself, is the one least likely to vary significantly in such a series. The other two perturbations, μ and R ,are a more direct reflection of the interactions of the ferric ion with its neighboring atoms in the molecule and vanish in the limit of the free ion. Thus, while one expects the spin-orbit coupling parameter to be somewhat sensitive to the local environment due to covalent bonding effects, these effects have been shown to create at the most a 20 % reduction in the free ion value when proceeding through a series of related prophyrin compounds (5).

It thus appears to be a reasonable assumption to fix the value of δ in this analysis. Then the parameter variation indicated in Fig. 2 *a* corresponds primarily to changes in the bonding interaction and local symmetry around the Fe atom. Fig. 2 *b* indicates the actual values of the other two parameters μ and R obtained for the fixed value of $\delta = 400\ \text{cm}^{-1}$. Proceeding across any row of this figure would indicate how a given property varies as both μ and R decrease for constant R/μ. Proceeding down any column headed by a constant value of δ/μ indicates the effect of increased rhombicity with the axial distortion remaining constant. We have calculated eigenfunctions and eigenvalues, g values, "zero field splittings" and values of μ_{eff}, the effective magnetic moment, as a function of temperature for the entire set of parameters given in Fig. 2 *b*. A given ratio of two parameters to a third uniquely determines the three eigenfunctions and the ground state g values. The unique set of g values so generated is given in Table III. The corresponding unique set of ground state wave functions is given in Table IV. The energy intervals, the so-called zero field splittings, are given in Table V. These are proportional to the value of δ chosen. The value of $\mu_{\text{eff}}(T)$ for three of the twelve temperatures calculated is given in Table VI. These values include thermal contribution from the two excited states. Since excited state energies depend on the value of δ chosen, the value of μ_{eff} also depends to some extent on the value of δ. In principle then, if energy or $\mu_{\text{eff}}(T)$ data were experimentally available for a set of compounds it would allow the determination of actual values of δ and how it varies in a series of compounds. However, the sensitivity of $\mu_{\text{eff}}(T)$ to changes in δ is not very great, as may be seen in Table VI, where sets of values of $\mu_{\text{eff}}(\delta)$ for $\delta = 200$, 300, and 400 is given.

TABLE

g VALUE VARIATION AS A FUNCTION

R/μ	δ/μ 0.01			0.02			0.04			0.1			0.2		
	g_x	g_y	g_z	g_x	g_y	g_z	g_x	g_y	g_z	g_x	g_y	g_z	g_x	g_y	g_z
0	0.020	0.020	4.00	0.040	0.040	4.00	0.080	0.080	4.00	0.198	0.198	3.97	0.383	3.90	3.90
0.01	1.40	1.43	3.42	0.858	0.934	3.79	0.406	0.564	3.94	0.098[-2]	0.395	3.96	0.285	0.481	3.90
0.05	1.96	1.98	2.39	1.84	1.90	2.74	1.51	1.64	3.26	0.711	1.08	3.78	0.102	0.857	3.86
0.1	1.99	2.01	2.20	1.95	2.00	2.39	1.83	1.94	2.75	1.27	1.61	3.42	0.532	1.26	3.73
0.2	2.00	2.02	2.10	1.98	2.03	2.20	1.95	2.04	2.40	1.71	2.00	2.91	1.13	1.77	3.40
0.4	2.00	2.02	2.05	2.00	2.03	2.10	1.98	2.06	2.20	1.90	2.12	2.49	1.63	2.14	2.90
0.5	2.00	2.01	2.04	2.00	2.03	2.08	2.00	2.06	2.16	1.93	2.13	2.40	1.73	2.20	2.75
1	2.00	2.01	2.02	2.00	2.03	2.04	2.00	2.05	2.08	1.97	2.13	2.20	1.90	2.24	2.39
2	2.00	2.01	2.01	2.00	2.02	2.02	2.02	2.04	2.04	2.00	2.10	2.10	1.97	2.20	2.20

TABLE

LOW SPIN GROUND STATE AS A FUNCTION

R/μ	δ/μ 0.01			0.02			0.04			0.1			0.2		
	A	$-C$	$-B$	A	$-C$	$-B$	A	$-C$	$-B$	A	$-C$	$-B$	A	$-C$	$-B$
0	1.0	0	0.007	1.00	0	0.014	1.00	0	0.027	0.998	0	0.067	0.992	0	0.125
0.01	0.924	0.381	0.006	0.973	0.228	0.013	0.992	0.120	0.027	0.996	0.047	0.067	0.991	0.022	0.125
0.05	0.774	0.633	0.005	0.829	0.559	0.011	0.903	0.429	0.024	0.973	0.220	0.064	0.986	0.112	0.124
0.1	0.742	0.671	0.005	0.774	0.633	0.010	0.830	0.558	0.022	0.926	0.371	0.060	0.970	0.212	0.121
0.2	0.726	0.689	0.005	0.742	0.670	0.010	0.774	0.632	0.020	0.854	0.517	0.054	0.926	0.361	0.113
0.4	0.716	0.689	0.004	0.724	0.690	0.008	0.742	0.670	0.017	0.790	0.610	0.046	0.855	0.510	0.100
0.5	0.714	0.700	0.004	0.721	0.693	0.008	0.735	0.677	0.016	0.775	0.630	0.043	0.832	0.547	0.091
1	0.711	0.704	0.003	0.714	0.700	0.007	0.721	0.692	0.013	0.742	0.669	0.093	0.775	0.627	0.072
2	0.709	0.705	0.002	0.710	0.703	0.005	0.715	0.700	0.010	0.724	0.688	0.025	0.742	0.668	0.052

Let us now consider the behavior of the g values as a function of axial and rhombic distortion. It might be mentioned that this analysis of g value behavior is independent of the actual choice of value for δ and of a small variation in δ as δ/μ or R/μ varies.

The region marked III A in Fig. 2 *a* is the near-octahedral limit where both μ and R are small compared to the spin-orbit coupling parameter. In most of this region, i.e., for R/μ less than 1, there are two g values somewhat less than 2 and one greater than 2. This is the observed esr behavior in some of the reduced plant-type ferredoxin which might then be in a near-octahedral environment at least as far as the localized, crystal field results indicate. We can analyze why such g values are obtained by considering the behavior of the interaction matrix of Table III as both R and μ approach zero. In such a case the only significant perturber and mixer of the states is the spin-orbit coupling. The 3×3 matrix then factors into a 2×2 and a

III

OF AXIAL AND RHOMBIC DISTORTION

0.4			0.5			1			5			10			100		
g_x	g_y	g_z	g_x	g_y	g_z	g_x	g_y	g_z	g_x	g_y	g_z	g_x	g_y	g_z	g_x	g_y	g_z
1.698	0.698	3.71	0.826	0.826	3.61	1.24	1.24	3.18	1.82	1.82	2.33	1.91	1.91	2.17	1.99	1.99	2.02
1.651	0.746	3.71	0.788	0.863	3.61	1.22	1.26	3.18	1.82	1.82	2.33	1.91	1.91	2.17	1.99	1.99	2.02
1.459	0.932	3.70	0.637	1.01	3.60	1.15	1.33	3.18	1.81	1.84	2.33	1.90	1.92	2.17	1.99	1.99	2.02
1.222	1.15	3.67	0.449	1.19	3.59	1.07	1.41	3.18	1.79	1.85	2.33	1.90	1.92	2.17	1.99	1.99	2.02
1.216	1.54	3.57	0.085	0.507	3.53	0.890	1.57	3.17	1.76	1.88	2.33	1.88	1.94	2.17	1.99	1.99	2.02
0.870	2.03	3.30	0.524	1.98	3.34	0.547	1.86	3.14	1.71	1.94	2.33	1.85	1.97	2.17	1.99	2.00	2.02
1.09	2.17	3.17	7.58	2.13	3.24	0.366	1.99	3.12	1.68	1.96	2.33	1.84	1.98	2.17	1.98	2.00	2.02
1.61	2.40	2.71	1.41	2.45	2.83	0.382	2.43	2.97	1.52	2.10	2.33	1.77	2.05	2.17	1.98	2.00	2.02
1.86	2.38	2.38	1.78	2.46	2.46	1.18	2.70	2.70	1.21	2.34	2.34	1.62	2.18	2.18	1.96	2.02	2.02

IV

OF AXIAL AND RHOMBIC DISTORTION

0.4			0.5			1			5			10			100		
A	$-C$	$-B$	A	$-C$	$-B$	A	$-C$	$-B$	A	$-C$	$-B$	A	$-C$	$-B$	A	$-C$	$-B$
1.976	0	0.218	0.967	0	0.255	0.929	0	0.369	0.850	0	0.527	0.834	0	0.552	0.818	0	0.575
1.976	0.010	0.218	0.967	0.008	0.255	0.929	0	0.368	0.850	0.003	0.527	0.834	0.003^{-1}	0.552	0.818	0.002^{-1}	0.575
1.975	0.052	0.218	0.966	0.040	0.254	0.929	0.018	0.369	0.850	0.003	0.527	0.534	0.001	0.552	0.818	0.001^{-1}	0.575
1.971	0.104	0.216	0.964	0.080	0.253	0.929	0.036	0.368	0.850	0.006	0.527	0.834	0.003	0.552	0.818	0.003^{-1}	0.575
1.957	0.198	0.211	0.956	0.157	0.249	0.927	0.072	0.367	0.850	0.011	0.527	0.834	0.006	0.552	0.818	0.005^{-1}	0.575
1.919	0.344	0.195	0.929	0.286	0.234	0.922	0.141	0.361	0.850	0.024	0.527	0.834	0.011	0.552	0.818	0.001	0.575
1.900	0.396	0.186	0.914	0.336	0.226	0.918	0.174	0.356	0.850	0.029	0.527	0.834	0.014	0.552	0.818	0.001	0.575
1.831	0.537	0.149	0.850	0.491	0.186	0.892	0.311	0.326	0.849	0.058	0.525	0.834	0.028	0.551	0.818	0.003	0.575
1.775	0.623	0.107	0.790	0.599	0.135	0.873	0.173	0.261	0.848	0.116	0.517	0.834	0.056	0.549	0.818	0.005	0.575

1×1 of the following form:

	ϕ_1	ϕ_2	ϕ_3
ϕ_1	$-\frac{1}{2}\delta - E$	$1/\sqrt{2}\delta$	0
ϕ_2	$1/\sqrt{2}\delta$	$0 - E$	0
ϕ_3	0	0	$+\frac{1}{2}\delta - E$

Solution of the 2×2 matrix yields two energies, $E = -\delta$ and $E = +\delta/2$. Thus in the limit of octahedral symmetry, spin-orbit coupling produces a two-component ground state with $E = -\delta$ and two accidentally degenerate excited states: the two-component partner of the ground state and the single noninteracting ϕ_3 state, both at energies of $+\frac{1}{2}\delta$. The energy intervals are $\Delta E_1 = \Delta E_2 = {}^3{}_2\delta$. The corresponding coeffi-

TABLE V

ZERO FIELD SPLITTINGS* AS A FUNCTION OF TETRAGONAL AND RHOMBIC DISTORTION

(δ = 400 cm^{-1})

R/μ	δ/μ	0.01		0.02		0.04		0.1		0.2		0.4		0.5		1		5		10		100	
		ΔE_1	ΔE_2	ΔE_1	ΔE_2	ΔE_1	ΔE_2	ΔE_1	ΔE_2	ΔE_1	ΔE_2	ΔE_1	ΔE_2	ΔE_1	ΔE_2	ΔE_1	ΔE_2	ΔE_1	ΔE_2	ΔE_1	ΔE_2	ΔE_1	ΔE_2
0		402	402[2]‡	404	202[2]	408	102[2]	418	423[1]	436	226[1]	463	132[1]	474	115[1]	512	825	576	632	587	614	599	602
0.01		568	403[2]	460	202[2]	420	102[2]	419	423[1]	436	227[1]	463	132[1]	474	115[1]	512	825	576	632	587	614	599	602
0.05		204[1]	412[2]	188[1]	205[2]	644	103[2]	464	426[1]	446	228[1]	466	132[1]	476	115[1]	513	825	576	632	587	614	599	602
0.1		402[1]	420[2]	204[1]	210[2]	108[1]	105[2]	589	430[1]	478	229[1]	473	133[1]	480	115[1]	513	825	576	632	587	614	599	602
0.2		800[1]	440[2]	402[1]	220[2]	204[1]	110[2]	900	447[1]	589	234[1]	502	134[1]	498	116[1]	516	828	576	632	587	614	599	602
0.4		160[2]	480[2]	801[1]	240[2]	402[1]	120[2]	165[1]	484[1]	905	250[1]	604	140[1]	564	120[1]	519	830	575	633	586	615	599	602
0.5		200[2]	500[2]	100[2]	250[2]	500[1]	125[2]	204[1]	504[1]	108[1]	259[1]	669	142[1]	608	122[1]	541	846	575	634	586	615	599	602
1		400[2]	600[2]	199[2]	300[2]	100[2]	150[2]	400[1]	603[1]	202[1]	308[1]	106[1]	165[1]	893	138[1]	615	914	573	641	585	619	599	602
2		798[2]	802[2]	390[2]	402[2]	198[2]	202[2]	782[1]	821[1]	384[1]	422[1]	188[1]	224[1]	151[1]	185[1]	824	111[1]	568	664	578	629	598	603

* In units of (cm^{-1}).

‡ Superscript n = $\times$ 10^n.

R/μ	T	δ/μ	0.01			0.04			0.1			0.2			0.5			1			10			100		
		δ	200	300	400	200	300	400	200	300	400	200	300	400	200	300	400	200	300	400	200	300	400	200	300	400
0	4		2.01	2.01	2.00	2.01	2.01	2.00	2.00	2.00	2.00	1.98	1.98	1.98	1.91	1.91	1.91	1.84	1.83	1.83	1.76	1.75	1.75	1.76	1.75	1.74
	77		2.22	2.17	2.13	2.22	2.17	2.13	2.24	2.17	2.13	2.25	2.17	2.13	2.25	2.15	2.09	2.25	2.13	2.05	2.25	2.10	2.02	2.25	2.10	2.01
	298		2.19	2.23	2.25	2.22	2.25	2.27	2.27	2.30	2.30	2.34	2.34	2.33	2.45	2.44	2.41	2.50	2.50	2.46	2.52	2.53	2.49	2.52	2.53	2.49
0.01	4		1.99	1.98	1.98	2.01	2.01	2.00	2.00	2.00	2.00	1.98	1.98	1.98	1.91	1.91	1.91	1.84	1.83	1.83	1.76	1.75	1.75	1.76	1.75	1.74
	77		2.12	2.07	2.05	2.22	2.16	2.13	2.24	2.17	2.13	2.25	2.17	2.13	2.25	2.16	2.10	2.25	2.12	2.05	2.25	2.10	2.02	2.53	2.10	2.01
	298		2.17	2.18	2.17	2.22	2.25	2.26	2.27	2.29	2.30	2.34	2.34	2.33	2.45	2.44	2.41	2.50	2.50	2.46	2.52	2.53	2.49	2.52	2.53	2.49
0.05	4		1.84	1.84	1.84	1.98	1..8	1.98	2.01	2.00	2.00	1.99	1.98	1.98	1.91	1.91	1.91	1.84	1.83	1.83	1.76	1.75	1.75	1.75	1.75	1.74
	77		1.87	1.86	1.85	2.10	2.06	2.04	2.21	2.15	2.11	2.24	2.17	2.12	2.25	2.15	2.09	2.25	2.13	2.05	2.25	2.10	2.02	2.25	2.10	2.01
	298		1.95	1.91	1.90	2.18	2.18	2.16	2.26	2.28	2.28	2.34	2.34	2.33	2.45	2.44	2.41	2.50	2.50	2.50	2.52	2.53	2.49	2.52	2.53	2.49
0.1	4		1.79	1.79	1.79	1.92	1.92	1.92	2.00	2.00	2.00	2.00	1.99	1.99	1.92	1.91	1.91	1.84	1.83	1.83	1.76	1.75	1.75	1.76	1.75	1.74
	77		1.81	1.80	1.80	1.98	1.96	1.95	2.15	2.10	2.07	2.22	2.16	2.12	2.25	2.15	2.09	2.25	2.13	2.05	2.25	2.10	2.02	2.25	2.10	2.01
	298		1.85	1.83	1.82	2.10	2.06	2.03	2.24	2.24	2.22	2.33	2.33	2.31	2.45	2.44	2.40	2.50	2.50	2.50	2.52	2.53	2.49	2.52	2.53	2.49
0.2	4		1.77	1.77	1.77	1.85	1.85	1.85	1.96	1.96	1.96	2.01	2.00	2.00	1.93	1.93	1.93	1.84	1.84	1.83	1.76	1.75	1.75	1.76	1.75	1.74
	77		1.77	1.77	1.77	1.89	1.87	1.87	2.04	2.02	2.00	2.17	2.12	2.09	2.24	2.15	2.09	2.25	2.13	2.06	2.25	2.10	2.02	2.25	2.10	2.01
	298		1.80	1.79	1.78	1.98	1.94	1.92	2.18	2.14	2.11	2.31	2.30	2.27	2.45	2.43	2.40	2.50	2.50	2.45	2.52	2.53	2.49	2.52	2.53	2.49
0.4	4		17.5	1.75	1.75	1.80	1.81	1.81	1.89	1.89	1.89	1.98	1.98	1.98	1.97	1.97	1.97	1.86	1.86	1.85	1.76	1.75	1.75	1.76	1.75	1.74
	77		1.76	1.75	1.75	1.82	1.82	1.82	1.94	1.92	1.92	2.08	2.04	2.03	2.22	2.14	2.10	2.25	2.13	2.06	2.25	2.10	2.02	2.25	2.10	2.01
	298		1.77	1.76	1.76	1.87	1.86	1.85	2.06	2.01	1.98	2.25	2.20	2.16	2.43	2.41	2.36	2.50	2.50	2.45	2.52	2.53	2.49	2.52	2.53	2.49
0.5	4		1.75	1.75	1.75	1.80	1.79	1.79	1.87	1.87	1.87	1.96	1.96	1.96	1.99	1.98	1.98	1.88	1.87	1.87	1.76	1.75	1.75	1.76	1.75	1.74
	77		1.75	1.75	1.75	1.81	1.81	1.80	1.91	1.90	1.90	2.04	2.02	2.00	2.20	2.13	2.09	2.24	2.13	2.06	2.25	2.10	2.02	2.25	2/10	2.01
	298		1.76	1.76	1.76	1.85	1.84	1.83	2.02	1.97	1.96	2.21	2.15	2.11	2.42	2.39	2.34	2.49	2.49	2.44	2.52	2.53	2.49	2.52	2.53	2.49
1	4		1.74	1.74	1.74	1.77	1.77	1.77	1.82	1.82	1.82	1.90	1.90	1.90	2.00	2.00	2.00	1.94	1.94	1.94	1.76	1.75	1.75	1.76	1.75	1.74
	77		1.74	1.74	1.74	1.78	1.78	1.77	1.84	1.84	1.84	1.94	1.93	1.92	2.13	2.09	2.06	2.22	2.13	2.08	2.25	2.10	2.02	2.25	2.20	2.01
	298		1.75	1.75	1.75	1.81	1.80	1.79	1.91	1.89	1.88	2.07	2.02	2.00	2.35	2.29	2.23	2.47	2.45	2.40	2.52	2.53	2.49	2.52	2.53	2.49
2	4		1.74	1.74	1.74	1.76	1.76	1.76	1.79	1.79	1.79	1.84	1.84	1.84	1.96	1.95	1.95	2000	2.00	2.00	1.76	1.75	1.75	1.76	1.75	1.74
	77		1.74	1.74	1.74	1.76	1.76	1.76	1.80	1.80	1.80	1.87	1.86	1.86	2.02	2.00	1.99	2.16	2.11	2.08	2.25	2.10	2.02	2.25	2.10	2.01
	298		1.74	1.74	1.74	1.78	1.78	1.77	1.85	1.84	1.83	1.95	1.93	1.92	2.20	2.13	2.09	2.40	2.35	2.29	2.52	2.53	2.49	2.52	2.53	2.49

cients of the ground state function are $A^2 = \frac{2}{3}$, $B^2 = \frac{1}{3}$, and $C^2 = 0$. We see from Table IV that these limiting values are indeed reached. In the last column of region III in Table IV $A = (\frac{2}{3})^{1/2} = 0.816$, $B = (\frac{1}{3})^{1/2} = 0.577$, and $C \sim 0$. When these values of A, B, and C are substituted into the expression for g_z, g_y, and g_x, one obtains the result that $g_z = g_y = g_x = 2$. Thus the g values, as is to be expected, are isotropic in the limit of octahedral symmetry, including spin-orbit coupling, and have a value of 2.

Having seen what happens in the octahedral limit, we can now discuss the remainder of region III A. For $R = 0$, the g value pattern is $g_x = g_y < 2$ and $g_z > 2$. As R increases from zero for constant axial distortion, g_x decreases, g_y increases and g_z remains approximately constant. This parameter variation then corresponds to a rhombic distortion which makes the x axis less like the z axis and the y axis more like it. With our convention, this means that as R increases, a D_{2h} trans-planar inequivalence among the prophyrin nitrogens is introduced and the interactions along the x axis are increasing and along the y axis are decreasing. In the limit of $R/\mu = 2$ for $\mu \leq \delta$, a new axial symmetry is reached. In this symmetry two g values are again equal, i.e., $g_y = g_z$ but these are greater than two while a new unique axis, the original x axis, is obtained along which the interactions are greater and the g value is less than 2. Thus maximum rhombic distortion occurs at some point between $R = 0$ and $R/\mu = 2$.

Let us now consider the strong axial limit, region I. For $R = 0$, the 3×3 matrix again factors into a 2×2 and a 1×1 matrix. However, for this limit, all off-diagonal elements are small compared to diagonal elements. Therefore there is very little mixing of any states, and the limit of single component state functions is reached. We see from Table IV that the ground state coefficients in region I A are indeed close to $A \simeq 1$, $B \simeq 0$, and $C \simeq 0$. In such a case we see from equations (2 *a–c*) for the g values that $g_z \simeq 4$, and $g_y \simeq g_x \simeq 0$. In this limit, then, the ground state would be esr inactive under the usual experimental conditions of an rf field perpendicular to the applied field. Indeed, no low spin, tetragonal esr spectra with $g_z = 4$ have ever been observed. As R increases in region I, the two inequivalent nearly zero values of g increase more or less together, never becoming very inequivalent. The g_z value decreases from 4 to a minimum value of 2. These variations are due to an increased mixing of the ϕ_3 function into the ground state, i.e., C increases while A and B decrease as R increases. Thus, the effect of increasing R starting from a very large axial perturbation seems to cause a conformation and bonding change which tends to make all three axes equivalent. This occurs by a decrease in the interactions along the x and y axes and a corresponding increase along the z axis. Thus a pseudo-isotropic limit is reached for large μ and R for which all three g values again appear to be 2, just as in the near-octahedral limit. In this strong axial, strong rhombic limit, however, the ground state wave functions are different. In the true octahedral limit we have seen that ψ_1 is approximately $\frac{2}{3}\phi_1$ and $\frac{1}{3}\phi_2$ with no ϕ_3 while in region I C ψ_1 is

approaching $\frac{1}{2}\phi_1$ and $\frac{1}{2}\phi_3$ with no ϕ_2. This limiting behavior is apparent from the A and C coefficients in region I C of Table IV where $C \to A \to \sqrt{\frac{1}{2}}$. In such a limit with these values of A, B, and C in the expressions for the g values, we find that again as in the octahedral limit but for different arithmetic reasons $g_x = g_y = g_z = 2$. There can be no greater than equal mixing of the ϕ_1 and ϕ_3 states, no matter how much the value of R is increased. Thus the limit of large values of R and μ corresponds to a different isotropic symmetry than near-octahedral limit.

Since the three g values are about equal to 2 both for large μ and R and small μ and R, a distinction between the region I C and III A for a given compound might be made on the basis of other properties. The zero field splittings, for example, should be quite different in the two cases. For the near-octahedral limit, region III A, $\Delta E_1 \simeq \Delta E_2 \simeq \frac{3}{2}\delta \simeq 600\ \text{cm}^{-1}$. For the region of large μ and R, these two energy intervals are unequal and approximately of the form $\Delta E_1 = (\delta^2 + R^2)^{1/2}$; $\Delta E_2 \simeq [\mu + (\delta^2 + R^2)^{1/2}/2]$, and since $R \gg \delta$, $\Delta E_1 \simeq R$, $\Delta E_2 = \mu + R/2$. These intervals will then be distinct and much larger than in the near-octahedral limit as can be seen from Table V. In region I C the zero field splittings are of the order of 10^4 with large differences between ΔE_1 and ΔE_2. In neither region III A or I C are the three doublet states close enough to interact appreciably in a magnetic field, or for an excited state esr to be seen. Therefore, only the direct measurement of the zero field splittings would distinguish them.

Another property which would help distinguish these two symmetry cases is the measured value of the effective magnetic moments as a function of T. As can be seen in Table VI, in the limit of large μ and R, the μ_{eff} value is 1.75 and is independent of temperature in the range 1–400°K. In the limit of very small μ and R, the low temperature value is again 1.75 but there is a substantial T dependence, the value increasing to 2.49 at room temperature. This behavior does not vary at all within each limiting region, nor is it very sensitive to variation in the value of δ. Hence, the difference in the T dependence of μ_{eff} in region III A and II C should be a measureable way to distinguish them.

Let us now consider region II of moderate axial distortions. In the limit of $R = 0$, there are two equivalent g values which are quite small and one larger distinct g_z value greater than 3. Again as for $R = 0$ and strong axial perturbation, the esr of compounds with this symmetry would be quite weak, though somewhat more allowed. In fact, no esr spectra of low spin ferric ion have been observed with two equivalent g values less than or close to 1 and one greater than 3. The only low spin $R = 0$ spectra which have been observed are those of the reduced plant type ferredoxins under some conditions.[2] For these both g values were close to 2.

As R increases through region II of moderate axial distortion, g_x and g_y increase but g_y more rapidly than g_x, and g_z decreases until a new axial symmetry is reached with $g_y = g_z > 2$ and $g_x < 2$. For moderate μ then, the effect of increasing R seems to be to weaken the interactions along the y axis and to strengthen those along the z

axis causing them to eventually become equivalent, while the interactions along the x axis appear to be even more strengthened, so that it becomes the unique axis with the lower value of g. For the smaller values of μ, i.e., in region III, as we have already discussed, the effect of R is different but the type of axial symmetry reached in the limit of $R > \mu$ appears the same.

To summarize then, in region I of large axial distortion, increasing rhombic distortion leads to a tetragonal and then to a pseudo-isotropic limit with all three g values equal to 2. In regions of moderate and weak axial distortion, one starts at zero rhombicity with an axial symmetry for which one g value is larger and two values are smaller than 2. For different reasons in each case, the effect of increasing R in these two regions is to produce a new axial symmetry with a new unique axis, the x axis. In such symmetry g_x is less than 2 while the two equivalent axes have g values greater than 2.

Finally we might comment on how the g values vary in going from the strong axial limit to the near-octahedral limit. Across any row in Table III μ and R decrease with a constant μ/R ratio. For $R = 0$, as we see from Table III, g_x and g_y increase together from 0 to 2 while g_z decreases from 4 to 2. As can be seen from the same row in Table IV, this is because as μ decreases states ϕ_2 and ϕ_1 increasingly interact and the coefficient of B in the ground state function increases at the expense of A. For $R \neq 0$ proceeding horizontally, g_x diminishes to a minimum and then increases to 2, g_y does the same only not to the same extent, while g_z increases to a maximum greater than 3 and then diminishes to 2.

The quantity $(g_y - g_x)$ is often taken as a measure of rhombicity. We have shown by our analysis of the way in which all three g values vary under different combinations of axial and rhombic perturbation that this is not a very good measure of "rhombicity". Specifically, in region I of strong axial symmetry at $R = 0$, $g_y - g_x)$ starts from zero, r aches a maximum and diminishes as R increases but is never appreciable. In moderate axial symmetry, this quantity has the same behavior with increasing R but becomes fairly appreciable near its maximum. Only for weak μ, i.e., $\mu \leq \delta$, does the quantity $(g_y - g_x)$ increase uniformly with increasing R. This is however because there is an exchange of unique axis in this process of increasing R.

Thus the behavior of $(g_y - g_x)$ is not monotonic with increasing R and is different depending on the ratio of δ/μ. It may be seen from Table III that a better criterion for increasing rhombicity would be that the maximum value of g decreases while the minimum value of g increases.

We have in the preceding discussion attempted to correlate g value behavior with variations in the values of the parameters μ and R. These parameters are clearly defined in terms of one-electron oribital energy differences given in Fig. 1. They are also defined in terms of the matrix elements of Table II B which establishes how they effect of the nature of the doublet states wave functions and therefore the g values and other properties associated with these states. These parameters are also linked

to the conformation and extent of perturbation of the local environment around the Fe. The crystal field potential establishes a formal link between them and the symmetry and extent of perturbation. Instead of proceeding with an analysis based on this formal link, we have shown how certain combinations of values and variations of μ and R correspond to certain actual conformational arrangements, i.e., the near-octahedral, pseudo-octahedral, "true" axial, and other axial symmetry limits as well as a maximum of true rhombic character for a middle region of the parameter range of R chosen. Thus we have established a three-way link between g value variation, parameter variation, and actual conformational and bonding-strength variations.

A SPECIFIC ANALYSIS OF THE FIVE TYPES OF LOW SPIN FERRIC HEME PROTEINS

Having thus analyzed the g value behavior of low spin ferric ion as a function of axial and rhombic distortions in general, we proceed to a specific analysis of the five types of ferric heme compounds listed in Table I. As seen from this table, the low spin esr of about 425 different heme proteins was observed.[1] As we have said, they fall into five different classes according to their g values. If, then, g values are taken as a direct indication of the symmetry and perturbation of the local environment about the Fe, it appears that among such similar compounds there can only be a finite number of inequivalent arrangements and bonding interactions. In all of these compounds the ferric ion is bonded to four in-plane nitrogens of a porphyrin ring, the defining structure of a heme group. In different heme proteins the substituents on the porphyrin ring can differ. In almost all heme proteins one of the axial ligands is an imidazole nitrogen of a histidine residue of the protein. In many, the sixth ligand position is occupied interchangeably to form a series of derivatives of the same protein. Many such derivatives for example, of hemoglobin itself, were investigated. In some of the heme proteins, the second axial position is also indigenous, being a part of another protein residue. For example, in cytochrome c the second axial ligand is a sulfur atom of a methionine residue. Any one of these chemical differences can also be accompanied by a conformation change. Yet with this possibility, it appears from this cataloging of esr results that only a limited number of conformations actually do occur. In our ensuing discussion of these results we take the plane of the four porphyrin nitrogens to be the xy plane and the z axis is defined as the non-porphyrin ligand axis perpendicular to that plane. The x and y axes are taken through pairs of porphyrin N ligands. The identification of these axes is retained through all the distortions of the porphyrin ring and variations of axial ligands that might be reasonably occurring in going through this series of compound types.

To account for the measured value of g for the five types listed in Table I, the experimental values of the g's were used in equations $2\,a$–c to determine the coefficients A, B, and C in the ground state function responsible for the observed resonance signal. Using these expressions plus the normalization conditions for the

coefficients, which overdetermines them, one option in the program written for the IBM 360/2040 allows an iterative search for the best set of ground state coefficients which satisfy all four conditions simultaneously. The ground state functions so obtained are given in Table VII A. Having thus determined these ground state functions, we then determined the ratio of δ/μ and R/μ to which they uniquely correspond. These ratios are also given in Table VII A together with our calculated g values to be compared with the experimental ones. Thus, with the variation in parameter ratios given, we have been able to explain all of the observed g values. Referring to the diagram given in Fig. 2 *a*, we see that all of these compounds are in the region of moderate axial and rhombic distortion where both R and μ are significantly greater than δ. This region is shown as the crosshatched rectangle in this figure.

The compound types are listed in Table VII A in order of decreasing value of g_z, the maximum g value, and increasing value of g_x, the minimum g value. As can be seen from this table, this monotonic g value variation does not correlate with a systematic variation in the ratio R/μ or δ/μ. However, if we make the reasonable assumption that the spin-orbit coupling constant does not change appreciably in going from one to the other type of similar heme protein and take a constant value of $\delta = 400\ \text{cm}^{-1}$, we can calculate actual values of μ and R. These values are also given in Table VII A. We see that these compounds are now listed in order of increasing value of R. This correlation agrees with that obtained in our general analysis of g value behavior: a measure of increasing rhombicity is decreasing g_z and increasing g_x. Also, in the series the tetragonal distortion is, in general, decreasing. Thus, they all belong in a small region of parameter space II B along a roughly diagonal path in the cross-hatched region shown in Fig. 2 *b*. By examining the coefficients of the ground state functions of these five types of compounds also given in Table VII A we see that as the rhombicity increases more ϕ_3 mixes with ϕ_1 approaching the limit of equal mixing. Also we see that the g value variation with increasing R corresponds to increased interaction along the z axis, decreased interaction along the x axis with relatively little effect on the interactions along the y axis.

Thus by the simple assumption of approximately constant spin-orbit coupling through this series of compounds we obtain a correlation between g value variation,

TABLE VIIA

CALCULATED g VALUES, SYMMETRIES, AND GROUND STATE WAVE FUNCTIONS FOR FIVE UNIQUE TYPES OF HEME PROTEINS

Type	g_z	g_y	g_x	δ/μ	R/μ	μ	R	A	$-B$	$-C$
c	3.10	2.21	1.23	0.373	0.527	1073	565	0.888	0.172	0.426
b	2.95	2.25	1.47	0.319	0.577	1254	723	0.864	0.144	0.482
h	2.79	2.26	1.66	0.259	0.605	1544	934	0.838	0.114	0.533
o	2.55	2.19	1.85	0.158	0.556	2531	1407	0.801	0.069	0.595
p	2.39	2.23	1.91	0.185	0.941	2162	2034	0.774	0.068	0.630

parameter variation, and possible conformational and binding changes. No other correlations give such clear results. For example, if we try to correlate g value variation with variation in the ratios of R/μ alone, we obtain no correlation whatsoever. The value of g_z and g_x vary erratically through the series with increasing value of R/μ. The two differences in the g values also show no clear trend. Nor does the variation in the separation of either of the extreme g values from the average of the other two show any trend. The uniqueness of our analysis of these compounds and this compatability with our general analysis gives us some confidence in the validity of the results.

From the wave functions which correspond to the observed g values we have also calculated the zero field splittings and temperature-dependent effective magnetic moments to be expected for these five types of compounds. The energy intervals are proportional to the actual value chosen for the spin orbit coupling while the ratio of the two intervals is not. Table VII B gives the value of the two energy intervals for $\delta = 400\ \text{cm}^{-1}$ and their ratio in the five types of compounds. We see from this table that as the rhombic character increases both energy intervals increase. However, except for the p-types, the ratio of the two energy intervals remains fairly constant in this series. These energy intervals correspond to differences in the one electron energies of the d_{xy}, d_{xz}, and d_{yz} orbitals. The different behavior of the p-type compound with the largest value of R might be due to the fact that it is proceeding towards another axial limit.

In Table VII B we have also given the value of the effective magnetic moment calculated at three different temperatures. At low temperatures, only the ground state is contributing significantly to the observed magnetic moment. Differences in the low temperature values in the different types of compounds are then a reflection of differences in their ground state wave functions. Since these functions correlate directly with observed g values, there should be a direct link between observed low temperature magnetic susceptibility and g values. Such measurements then would provide another check on the validity of the proposed model for explaining observed g values. Since the energy intervals are rather large in all five types of compounds,

TABLE VIIB

CALCULATED VALUES OF ZERO FIELD SPLITTING AND EFFECTIVE MAGNETIC MOMENTS FOR FIVE LOW SPIN TYPES OF HEME PROTEINS

Type	Zero field splitting			$\mu_{eff}(T)$		
	ΔE_1	ΔE_2	$\Delta E_1/\Delta E_2$	4.2°	77°	295°
c	716	1527	0.47	2.00	2.08	2.27
b	841	1761	0.47	2.00	2.06	2.21
h	1021	2128	0.47	1.98	2.02	2.14
o	1463	3310	0.44	1.92	1.95	2.03
p	1909	3063	0.62	1.89	1.92	1.99

not too large a temperature variation is calculated in the T range 1.5–400°K. However, the temperature dependence does become more pronounced as the intervals decrease, i.e. the rhombic and tetragonal distortions decrease, through this series of five types. Thus the predicted temperature dependence can serve as an additional check on this model as corresponding experimental data begins to accumulate.

The author wishes to thank Drs. William Blumberg and Jack Peisach for use of their data and many helpful discussions.

She also wishes to gratefully acknowledge the partial support of NSF grant No. GB 5215 in funding this work.

Received for publication 13 June 1969.

REFERENCES

1. HARRIS, G. 1966. *Theor. Chim. Acta.* **5**:379.
2. HARRIS, G. 1968. *Theor. Chim. Acta.* **10**:119.
3. HARRIS, G. 1968. *Theor. Chim. Acta.* **10**:155.
4. HARRIS, G. 1968. *J. Chem. Phys.* **48**:2191.
5. ZERNER, M., and M. GOUTERMAN. 1966. *Theor. Chim. Acta.* **4**:44.